

Applications of Magnetic Torque to Various Static and Dynamic Experiments

Jeff Lam, Victoria Herrada

Department of Physics, Binghamton University

May 4th, 2025

Abstract

The M τ 1-A instrument designed by TeachSpin Inc. applies the concept of magnetic torque across three possible experiments: (1) *Magnetic vs. Gravitational Torques*; (2) *Harmonic Oscillation of a Spherical Pendulum*; and (3) *Precessional Motion of a Spinning Sphere*, where (1) is a form of static experiment and (2) & (3) are forms of dynamic experiments. In all cases, the magnetic dipole moment μ of a neodymium magnetic can be determined through careful data collection on the strength of the generated external magnetic field, applicable parameters when the experiment calls for them such as the housing cue ball's diameter, mass of the cue ball, *etc.*, and timings of periodic motion for the dynamic experiments. Linear least-squares fitting is applicable across all three experiments, and for every model a predictive slope parameter a can be calculated to help derive experimental values of μ from theoretical relationships established for each experiment. These relationships were determined to be $a \propto \frac{mg}{\mu}$, $a \propto \frac{4\pi^2 I}{\mu}$, and $a \propto \frac{\mu}{L}$ for measurable values B , T , and Ω_p with respect to each experiment, where I is moment of inertia of a sphere, L is large spin angular momentum of a rotating cue ball, T is oscillation period of the spherical pendulum, and Ω_p is precessional period of the spinning sphere. For an accepted μ value of $0.4 \text{ A} \cdot \text{m}^2$, the experiments yielded values with percent errors of 4.5%, 24.65%, and 46.44%. The increasing percent error values likely is due to dismissal of small angle approximation for the dynamic experiments when carried out.

1 Introduction

Electric motors capable of converting electrical energy to mechanical energy are the most common application involving torque— in all cases, however, an external magnetic field is almost always necessary. This is typically done via two ways when given a loop of current: (1) using a split-ring commutator to essentially produce Alternating Currents (AC) if the external magnetic field is constant in one direction; or (2) producing AC magnetic fields if given a Direct Current (DC) loop (typically then the magnetic field is supplied by AC coils as electromagnets). Nevertheless, the torque produced by these scenarios

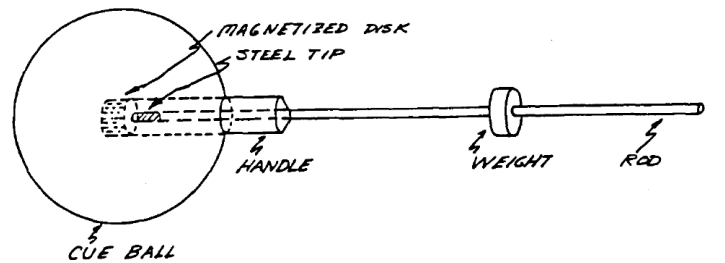


Figure 1: Schematic diagram of M τ 1-A's cue ball.

is due to an external magnetic field and the loop of wire acting as a magnetic dipole.

While the experiments outlined by this paper essentially only apply magnetic torque for a single moment (*i.e.*, no AC applications for continuous rotation), there are rich static and dynamic procedures

that can be followed to experimentally determine a magnetic dipole moment within an external magnetic field. In this paper, the theory and laboratory procedures of three experiments were explored:

Part I: Magnetic vs. Gravitational Torques

Part II: Harmonic Oscillation of a Spherical Pendulum

Part III: Precessional Motion of a Spinning Sphere

2 Setup Specifications

All experiments were designed by TeachSpin Inc., and furthermore, the instrument used to carry out these experiments was also provided by them. This instrument is referred by TeachSpin as “MAGNETIC TORQUE M τ 1-A”—in this paper it is simply referred to as M τ 1-A. Provided by the kit are a few specially tailored parts.

2.1 The Cue Ball

Figure 1 is a provided schematic diagram of what TeachSpin dubs the “cue ball” for their M τ 1-A, along with other specifications in which the majority were used in *Part I* of the experiments. As it can be seen, the core of the cue ball houses a magnetized disk, specifically a Nd₂Fe₁₄B (neodymium iron boron) permanent magnet, *a.k.a.* a neodymium magnet, which initially seems to contradict the introduction of magnetic torque as usually involving a loop of current as the magnetic dipole. However, TeachSpin assures that the permanent magnet is magnetized such that the magnetic field produced is along the axis of the handle as shown in the figure, acting as if it was an ideal magnetic dipole.

2.2 M τ 1-A

The overall objective across all three experiments designed by TeachSpin is to experimentally derive



Figure 2: Provided image from a brochure titled “Magnetic Torque: A ‘Classic’ Made Even Better”, featuring M τ 1-A. More features of M τ 1-A can be seen as a set of Helmholtz coils, an air bearing, a strobe light, and a control box to tune every one of them [1].

a value for the magnetic dipole moment of the neodymium magnet from various applications of magnetic torque. **Figure 2** provides a photograph showcasing the rest of the M τ 1-A instrument. According to the included reference as well, M τ 1-A comes with a pair of Helmholtz coils made out of 195 turns of #18 copper wires, an air bearing at the center which is also specifically designed such that the cue ball is raised to house the neodymium magnet at the center of the coils, a strobe light for assistance in carrying out experiment *Part III*, and a control box which also houses an air pump and power supply for the platform. Some important notes of these specifications is that the Helmholtz coils help produce a uniform magnetic fields [2] and the air bearing helps ensure minimum friction between the cue ball and bearing socket—an observer may then assume it being negligible across all experiments.

Some things to note from the specifications provided by the reference is first a detail that the *magnetic moment of the magnetized disk should measure as $0.4 \text{ A} \cdot \text{m}^2$* —this value act as the accepted answer across all experiments done in this paper. From both the included reference and the M τ 1-A lab manual, the magnetic field supplied by the Helmholtz coils were appreciably calculated by TeachSpin as $B = 1.36 \pm 0.03 \times 10^{-3} \text{ T/A}$ —these values assist in determining the strength of the B field for a given

current reading throughout section 4 **Methods and Data Analysis** (and the uncertainty values were especially used for the least-squares fitting for *Part I* of the experiments).

3 Theory

3.1 The Theory Behind Part I

Figure 3 helps demonstrate the theoretical setup for balancing magnetic and gravitational torques. In many introductory physics II curriculums, it can be shown that for a magnetic moment μ within an external magnetic field B , the torque produced by the misalignment of the two vectors can be evaluated via the cross product $\tau = \mu \times B$, where τ is a pseudovector representing torque. Because the definition involves the cross product, the direction of τ can be determined via the right-hand rule— curling one's fingers starting from the vector representing μ to the vector representing B . The right-hand rule is also the reason why torque due to a magnetic dipole moment τ_B is a vector pointing outside of the page, as confirmed by the figure.

If one were to attached the aluminum rod (assumed to be massless) and furthermore attach the disk carrying a mass m at a distance r away from the cue ball's center of mass, a second torque would be produced due to gravity. The formula for the torque produced by this setup can also be derived from any typical introductory physics I curriculum, given as $\tau = r \times mg$. The right-hand rule may also be used in this scenario to determine the direction of τ_g the torque due to gravity as pointing inside of the page— this is also confirmed by the figure.

Because τ_B and τ_g points opposite to each other, Newton's First Law of Motion for rotational kinematics may be applied if the system is setup such that no net torque acts on the system, *i.e.*, $\tau_B = \tau_g$. From there it can be shown that

$$\mu \times B = r \times mg \longrightarrow \mu B \sin(\theta) = rmg \sin(\theta)$$

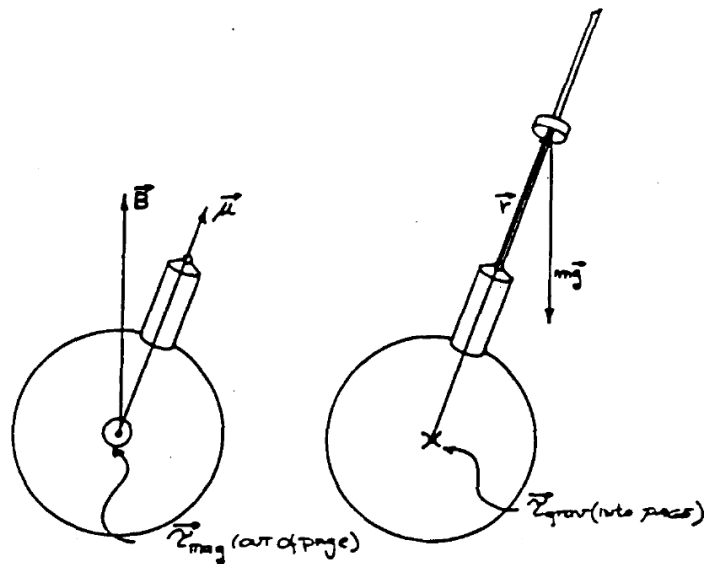


Figure 3: Schematic setup of the theory behind balancing magnetic and gravitational torques from the M71-A's manual.

where θ represents the angle spanned from the cross product of either side. Choose the balance of the system to be when the aluminum rod is horizontal. Then $\theta = \frac{\pi}{2} \rightarrow \sin\left(\frac{\pi}{2}\right) = 1$. From this relationship, one may derive a formula for B as $B = \frac{mg}{\mu}r$, allowing one to derive an experimental linear slope from a least-squares fitting to derive a value for μ . It is worth noting that the relationship derived in this step departs from what was provided from M71-A's lab manual (where it was instead derived as $r = \frac{\mu}{mg}B$), for a different experimental procedure was followed when gathering data.

3.2 The Theory Behind Part II

Because this and *Part III* of the experiments are dynamics, Newton's Second Law of Motion for rotational kinematics may be applied. Take Newton's Second Law in the form of $\sum \tau = \frac{dL}{dt}$, analogous to force being the time derivative of momentum in translational kinematics. It was already provided that the torque τ due to a uniform magnetic field can be expressed as $\mu \times B$. However, consider the scenario again where μ is misaligned with the external magnetic field B : the torque produced from the mis-

alignment will act such that it would move *against* the angular displacement of μ , *i.e.*, the torque is a *restorative* torque, analogous to how spring force is a restorative force in translational kinematics. Then Newton's Second Law in this scenario may be expressed as

$$-\mu \times B = \frac{dL}{dt}$$

Use the definition of cross product on the left-hand side and the definitions $L = I\omega$ and $\omega = \frac{d\theta}{dt}$ on the right-hand side to further express the differential equation as

$$-\mu B \sin(\theta) = I \frac{d^2\theta}{dt^2}$$

Take $\sin(\theta) \approx \theta$ for small angular displacements between the dipole moment and the direction of the uniform magnetic field. Then the expression $-\mu B \theta = I \frac{d^2\theta}{dt^2}$ may be solved as simple harmonic motion:

$$\theta(t) = A \cos(\omega t)$$

where $\omega = \sqrt{\frac{\mu}{I} B}$. If one were to instead measure periods of oscillation rather than angular frequency, then the definitions $\omega = 2\pi\nu$, $\nu = \frac{1}{T}$ closes a form of the period for the cue ball acting as a spherical pendulum moving under simple harmonic motion as

$$T^2 = \frac{4\pi^2 I}{\mu} \frac{1}{B}$$

where in this scenario, moment of inertia I is taken as $\frac{2}{5}mr^2$ for the mass m and spherical radius r of the cue ball. Similarly to experiment *Part I*, a linear least-squares fitting model can help produce an experimental slope value to determine μ .

3.3 The Theory Behind Part III

Precession is defined as the change in orientation of a rotating body's axis of rotation. Precession in fact occurs within Earth's rotation, in which its effect manifests as the reason why some seasons are more

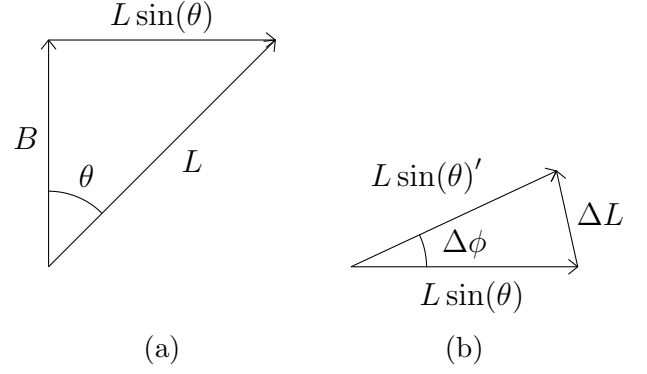


Figure 4: Trigonometric relationships for proving precessional angular velocity as $\Omega_p = \frac{\mu}{L} B$. (a) represents a side view of the spinning tilted cue ball, where L points at the same direction as the axis tilt, and (b) represents a top view of when the large spin angular momentum L changes due to a weak torque.

extreme in one hemisphere than another [3].

Start with the result of applying Newton's Second Law from the last section, $\mu \times B = \frac{dL}{dt}$, but this time L represents the spin angular momentum of the rotating body (*i.e.*, the cue ball spinning). **Figure 4** will help visualize how precession motion arises. From **4a**, it can be seen that L points in the same direction as the axis tilt—to measure the precessional angular displacement, a top arrow representing $L \sin(\theta)$ is drawn. The transition to **4b**, a top view of the rotating object now, showcases how a small change in angular momentum ΔL is caused by a small change in precessional angular displacement $\Delta\phi$ due to a weak torque [4]. Since these changes are small, the resultant vector can be well-approximated as an arc via the formula $s = r\phi$. Then the change in spin angular momentum can be expressed as $\Delta L = \Delta\phi L \sin(\theta)$. Take this over a small change in time Δt and take the limit as Δt approaches to zero:

$$\lim_{\Delta t \rightarrow 0} \frac{\Delta L}{\Delta t} = \frac{\Delta\phi}{\Delta t} L \sin(\theta)$$

It is now appropriate to substitute these definitions in differential form. Then the change in angular mo-

mentum over time is precisely

$$\frac{dL}{dt} = \Omega_p L \sin(\theta)$$

where Ω_p is the precessional angular velocity.

Take again the definition of cross product on the left-hand side of the result of Newton’s Second Law, and substitute the definition of $\frac{dL}{dt}$. It can be further simplified to

$$\mu B \sin(\theta) = \Omega_p L \sin(\theta) \longrightarrow \mu B = \Omega_p L$$

where the mutual $\sin(\theta)$ terms on either side cancel each other out. Finally, a derivable relationship for Ω_p can be given as $\Omega_p = \frac{\mu}{L} B$. Once again, a linear least-squares fitting model on an appropriately gathered data set will yield a slope term to express a value for μ

4 Methods and Data Analysis

All data gathered can be viewed in **Appendix A: Data Gathered Across All Experiments**.

4.1 Magnetic vs Gravitational Torques

This is *Part I* of the experiments designed by Teach-Spin. The mass of the attachable disk m was weighed in as 1.367 g and the diameter of the cue ball was measured as 5.334 cm using a caliper (so the radius is measured as 2.667 cm). Additionally, the length of the handle was measured as 1.25 cm using a precession ruler[†]. The aluminum rod as shown before in **Figure 1** was plugged into the handle, and in the same figure it can be seen that some of the rod’s length gets embedded. Using a marker, an initial tick was marked at where the handle ends on the rod, then various 1 cm ticks were marked from that point towards the other end of the rod. In total, eight 1 cm tick markers were introduced, but as it

[†]Note: measuring the handle in the laboratory was a bit tricky since the cue ball is a bulky object itself, and most rulers do not start measuring from their end—the measurement was taken *with perspective* to correctly offset the ruler’s starting measures.

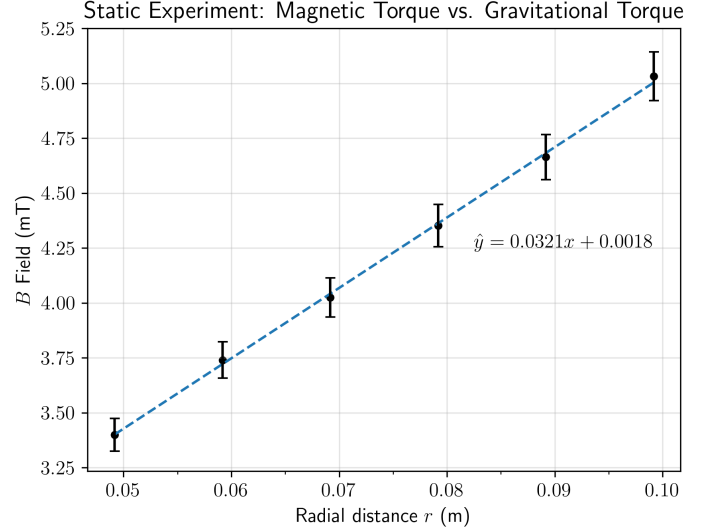


Figure 5: Scatterplot of experiment *Part I: Magnetic vs. Gravitational Torques*. Error bars represent the uncertainty of the B field supplied by the Helmholtz coils scaled by the amount of current flowing through the system. Uncertainties in the predictive parameters a, b were significantly low that they are not shown in the graph.

can be seen in **Appendix A**, the existence of only six rows in **Table 1** implies only data for the first six tick markers could be collected. When the attachable disk was set on the first two markers from the rod’s farthest end, not even the maximum current i that could be supplied (4 A) could create enough torque to counteract the gravitational torque due to the disk’s weight (*i.e.*, it was only at the 6 cm mark did the attachments lift).

The general procedure for gathering data follows by starting the air pump and turning on the magnetic field in the “UP” direction. For every tick marker, the current supplying the Helmholtz coils were “tuned” via the current knob beneath the ammeter as shown in **Figure 2** until the attached aluminum rod and disk lifts to a horizontal position. During the process, the system may oscillate—in these scenarios an observer temporarily held the system to help stabilize it from the motion before further tuning. Once an appreciable horizontal position

of the rod and disk was achieved, the ammeter reading was recorded. The ammeter of M τ 1-A has major ticks for every 1 A and minor tick markers for every 0.5 A—the needle whenever it was between the ticks was approximated as some in-between value for recording. Between each trial for each tick marker, the Helmholtz coils were monitored for their temperatures, as hot coils could affect the readings from a weaker magnetic field.

Figure 5 shows the data gathered for *Part I* of the experiment graphed alongside its least-squares fitting. The tick markers measuring in 1 cm, 2 cm, ..., 6 cm had the radius of the cue ball and the length of the handle added to achieve the total radial distance r from the center of masses between the cue ball and attachable disk. The strength of the B field for each current reading was determined using the value introduced from section 2.2 M τ 1-A. For this experiment only, a weighted least-squares fitting model using the uncertainty of the B field per Amp of current value given. For the predictive slope parameter a , $a \propto \frac{mg}{\mu}$, and by substituting the appropriate values μ for this experiment was approximated as $0.418 \text{ A} \cdot \text{m}^2$. The results of this experiment remarkably yielded a percent error of 4.5% only, which demonstrates the straightforward yet robust method of this experiment regarding measuring the value of μ . However, as it will be shown soon, the same cannot be said for the other parts of the experiment.

4.2 Harmonic Oscillation of a Spherical Pendulum

For this part of the experiment, the only measurable value that needed to be determined was the weight of the cue ball. The mass of the cue ball m was measured to be 0.142 kg using a scale. Like with the previous experiment, the air pump and Helmholtz coils were turned on, starting with a current supply of 0.5 A. With the cue ball sitting in the air bearing, the handle was given an initial angular displacement before letting go, setting the object off to simple harmonic motion. 20 oscillations of the motion was

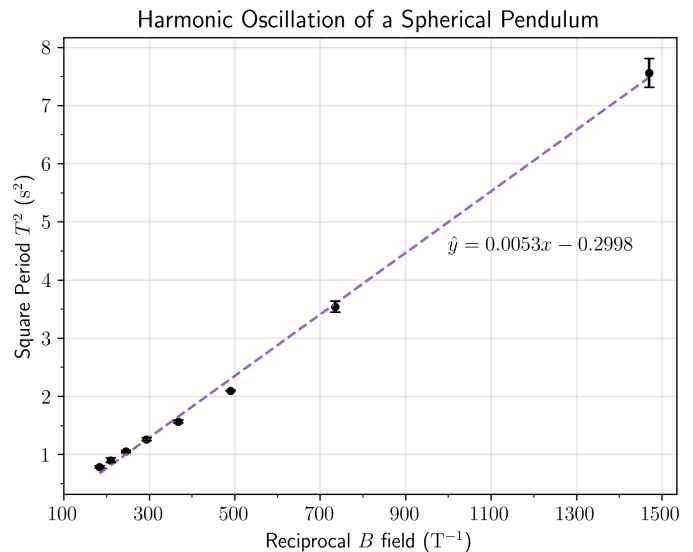


Figure 6: Scatterplot of experiment *Part II: Harmonic Oscillation of a Spherical Pendulum*. Error bars represent the standard deviation of the three trials carried out for each oscillation timing of a given current reading. Like with *Part I* of the experiments, uncertainties in the predictive parameters a , b were significantly low, hence they are not reported.

timed before repeating the procedure for the next 0.5 A reading, up to the maximum 4 A that can be supplied. A total of three trials were carried out to account for variation in the least-squares fitting model.

Figure 6 shows the data gathered for *Part II* of the experiment graphed alongside its least-squares fitting. The timing data was first converted to period of oscillations by simply dividing 20 for the count of oscillation observed, then *squared* since the relationship determined in section 3.3 *The Theory Behind Part II* was determined as $T^2 = \frac{4\pi^2 I}{\mu} \frac{1}{B}$. Similarly as the relationship is shown here, the *reciprocal* of the B field readings were taken to properly allow the predictive slope parameter a in the experiment to represent the grouped term being shown. For the predictive slope parameter a , $a \propto \frac{4\pi^2 I}{\mu}$. As mentioned in the section 3.3, moment of inertia of the object can be calculated by assuming the cue ball to be a sphere with uniform mass density, $I = \frac{2}{5}mr^2$.

The mass value and the radius value determined in the previous section was used as appropriate substitutions to approximate the value of μ as $0.301 \text{ A} \cdot \text{m}^2$. Unlike the near precise experimentally determined value of μ in the previous section, the μ value determined here suffers about a 24.65% error.

4.3 Precessional Motion of a Spinning Sphere

No additional measurable value were needed for *Part III* of the experiments. The air pump of M τ 1-A was turned on, but this time *no current was supplied yet*— a measurable large spin angular frequency must first be set to cue ball alongside a tilt. It has not been mentioned so far that near the hole of the handle where the attachable rod can be plugged in is there a reflective white dot. The use of the white dot and the strobe light helped set the cue ball in a tilted spin frequency of a known value. And so, the lights of the laboratory was turned off, and the strobe light was turned on, setting it at a value of 4.5 Hz. The cue ball sitting on the air bearing was given a large body spin— multiple attempts and re-sets were necessary for a bad spin could make the object wobble.

When a stable spin was achieved, an observer would use *the tip of their finger* to help guide the spinning end of the handle to face the direction of the strobe light— this also tilted the rotating object at approximately 45° . With the lights out and strobe light on, the spin frequency of the cue ball can be viewed as a form of stop-motion effect. It can be intuitively understood that if the white dot on the handle is visible to the observer at one spot, then the cue ball is spinning at the same frequency as the strobe light. Likely, when initially viewing the white dot under the strobe light, it is appearing across multiple places on the end of the handle.

An observer would wait until the white dot seemingly settle at a point before quickly turning on the magnetic field to a starting current of 1 A (quickly because the frequency of the ball's spin *does change*

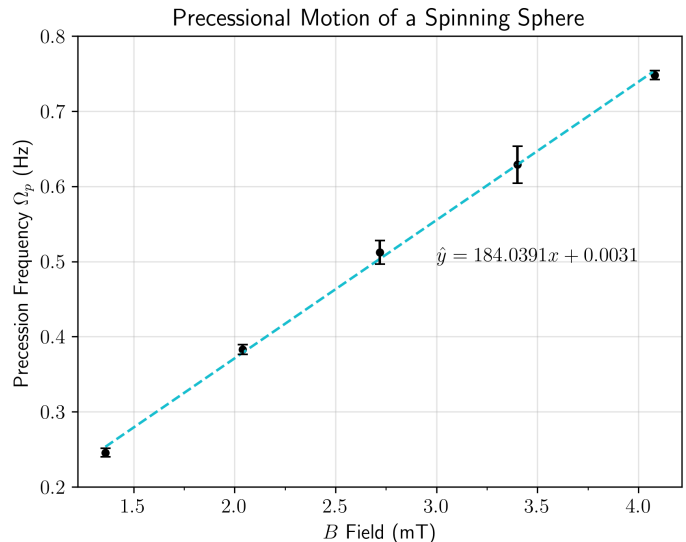


Figure 7: Scatterplot of experiment *Part III: Precessional Motion of a Spinning Sphere*. Error bars represent the standard deviation of the three trials carried out for each one precessional period timing of a given current reading. Unlike the other least-squares fitting models, uncertainties found here are no longer significantly low such that they can be neglected: the uncertainty values for the parameters a , b were $\pm 3.708 \text{ T}$ and $\pm 0.011 \text{ T}$, respectively, reported in the form of standard error.

over time, as a form of exponential decay). After carefully tuning the magnetic field to the desired current supply, the observer quickly looks back at the cue ball and times how long it takes for the object to do *one* precession around where the handle was first seen oriented. Afterwards, the current was turned off and the cue ball was set at rest for the next measurement. This procedure was repeated for the next 0.5 A readings, up to ideally the maximum 4 A that M τ 1-A can supply, however data could only be gathered up to 3 A for further attempts in measuring precession period at current readings higher than this introduced strong *nutations* to the rotating object, making it more difficult and therefore unreliable to time its precession period. Like with *Part II* of the experiment, three trials were carried out to account for variation in the least-squares fitting model.

Figure 7 shows the data gathered for *Part III* of the experiment graphed alongside its least-squares

fitting. The precessional period data can be converted to precessional frequency in Hz via dividing 2π with each data point (a similar conversion was used in section 3.2 *The Theory Behind Part II*). And like *Part I* of the experiment, the current readings where each data point were gathered can be converted to B field strength using the value introduced in section 2.2 *M71-A*. For the predictive slope parameter a , $a \propto \frac{\mu}{L}$. The large spin angular momentum L can be calculated using the definition $L = I\omega$, where I is the moment of inertia of the cue ball calculated previously and ω is angular frequency determined via simply multiplying 2π to 4.5 Hz. The results of the experiment yielded a μ value of $0.210 \text{ A} \cdot \text{m}^2$, a significantly worse result than what was concluded in *Part II* of the experiments, suffering a percent error of 47.44%.

5 Conclusion

Overall, the M71-A instrument designed by Teach-Spin introduces exciting experiments to explore various applications of magnetic torque. Out of the three experiments designed by them, the first one seemed straightforward enough that it yielded correct results, while the other two can be considered significantly harder to do the same. Likely avenues of errors introduced that could explain how the μ values begin to differ are for *Part II* of the experiments, too large of an angular displacement was set for every reading (very similarly to the Coupled Pendulums Experiment), and for *Part III* of the experiments, a similar conclusion follows: too large of a tilt angle likely interfered with the precession and may even likely be the cause behind the nutation at current readings greater than 3 A.

References

- [1] Magnetic Torque, *TeachSpin, Inc.*, <https://www.teachspin.com/magnetic-torque>
- [2] Richtberg, Stefan. Magnetic field of two Helmholtz coils, *Ludwig Maximilian University of Munich*, <https://virtuelle-experimente.de/en/b-feld/b-feld/helmholtzspulenpaar.php>
- [3] NASA Science Editorial Team, Milankovitch (Orbital) Cycles and Their Role in Earth's Climate, *NASA*, <https://science.nasa.gov/science-research/earth-science/milankovitch-orbital-cycles-and-their-role-in-earths-climate/>
- [4] Taylor, John R. *Classical Mechanics* (University Science Books, 2003), p. 392

Appendix A: Data Gathered Across All Experiments

Table 1: Current tuning for various distances of r

Current i (A)	B Field (T)	Radial distance r (m)
2.5	0.0034	0.04917
2.75	0.00374	0.05917
2.96	0.00403	0.06917
3.2	0.00435	0.07917
3.43	0.00466	0.08917
3.7	0.00503	0.09917

Table 2: Timings of 20 oscillations for the spherical harmonic pendulum

Current i (A)	Trial 1 (s)	Trial 2 (s)	Trial 3 (s)
0.5	53.98	55.21	55.76
1.0	37.16	37.53	38.19
1.5	28.91	28.97	28.94
2.0	24.77	25.15	25.12
2.5	22.25	22.69	22.42
3.0	20.51	20.33	20.66
3.5	18.6	19.39	18.87
4.0	17.56	17.93	17.71

Table 3: Timings of precessional periods for a spin frequency of 4.5 Hz and tilted at 45°

Current i (A)	Trial 1 (s)	Trial 2 (s)	Trial 3 (s)
1.0	26.19	25.0	25.6
1.5	16.1	16.66	16.46
2.0	11.86	12.57	12.38
2.5	9.85	9.7	10.45
3.0	8.32	8.42	8.45